Effect of gold layer thickness on optical properties and sensing performance of triangular silver nanostructure array

JING LIU[a,b,c,*], HAOYUAN CAI[a], LINGQI KONG[b,c]
School of Information Engineering, Jimei University, Xiamen, Fujian 361021, PR China
Department of Physics, Xiamen University, Xiamen, Fujian 361005, PR China
China–Australia Joint Laboratory for Functional Nanomaterials, Xiamen University, Xiamen, Fujian 361005, PR China

Optical performance of the nanophotonic devices with pure silver nanostructure will be changed due to the oxidation and sulfuration. A hybrid Au-Ag triangular nanostructure is put forth for the purpose of preventing oxidation and sulfuration of Ag film. Effect of gold layer thickness on optical properties and sensing performance of the hybrid nanostructure array is systematically investigated through numerical simulation using the discrete dipole approximation (DDA) method. Theoretical results show that the oxide layer and sulfide layer leads to a significant red shift in the localized surface plasmon resonance (LSPR) λ_{max}. The refractive index sensitivity (RIS) and figure of merit (FOM) of the hybrid nanostructure array strongly depend on thickness of the Au layer. It is found to possess the better RIS and FOM, when thickness of Au is 10 nm, thickness of Ag is 25 nm. Moreover, the hybrid nanostructure with the suitable Au layer thickness is fabricated by nanosphere lithography (NSL). The experimental results demonstrate that the measured spectrum is basically in agreement with the theoretical spectrum derived by the DDA calculation.

1. Introduction

Noble metal nanostructures are well known for their ability to exhibit localized surface plasmon resonance (LSPR). The LSPR phenomenon of nanostructures has been applied as materials for surface-enhanced spectroscopy [1], optical filters [2], plasmonic devices [3, 4], and sensors [5]. However, most of them are designed on the basis of silver thin film metallic nanostructures.Corrosion-induced electrochemical damage on surface of the Ag film exists at ambient atmosphere, especially in the period of time after micro/nanofabrication. The corrosion originates from oxidation and sulfuration which is well known for bulk Ag. But the relative permittivity of the Ag thin film will be definitely changed due to the oxidation and sulfuration. The optical performance of the nanophotonic devices will vary accordingly.

To overcome this problem, many researchers have put forth a hybrid Au-Ag nanostructure array with gold thin film covered on the Ag film surface. The Au film can protect oxidation and sulfuration of the pure Ag particles from ambient environment and tune the plasmon peak. The study of the hybrid Au-Ag nanostructure array has become very appealing for many researchers. For example, J.Y. Liu

et al. [6] investigates the extinction spectra and refractive index sensitivity (RIS) of the hybrid Au-Ag quadrangular frustum pyramid nanostructure. Y. Q. Fu et al. [7] introduces a hybrid Au-Ag subwavelength metallic zone plate-like structure and shows that thickness of both the Au and Ag thin films has significant tailoring function. In addition, S.L. Zhu and W. Zhou [8] also focus on the study of the period and RIS of the hybrid Au-Ag rhombic nanostructure. To the concern of our knowledge, there are no works investigating the effect of Au layer thickness on optical properties and sensing performance of triangular Ag nanostructure array. The RIS and figure of merit (FOM) of the LSPR sensor [9-14] are sensitive to the thickness of the Au layer, so the influence of the Au layer thickness on optical properties and sensing performance of the hybrid nanostructure is important as the main topic of this paper.

In this paper, a hybrid Au-Ag triangular nanostructure is put forth for the purpose of preventing oxidation and sulfuration of Ag film. The extinction spectra of the oxidation and sulfuration of triangular Ag nanoparticles are calculated by discrete dipole approximation (DDA) and they all are compared with that of triangular Au-Ag nanoparticles with different Au layer thicknesses. This results suggest that the hybrid Au-Ag triangular nanostructure is a good structure to tune the plasmon peak.

Moreover, we calculate the RIS and FOM of the hybrid nanostructure arrays with different Au layer thicknesses. According to the calculated results, the hybrid nanostructure array with the suitable Au layer thickness is fabricated by nanosphere lithography (NSL).

2. DDA method

The DDA method provides a convenient method for describing light scattering from nanoparticles of arbitrary shape. In the DDA formalism, the object of interest, usually called "target", is described as a cubic array lattice of electric dipoles (N-point dipoles) in which the polarizability and position vector of each dipole are specified as α_i and r_i, respectively. The induced dipole polarization P_i in each element is determined from [15-18]

$$P_i = \alpha_i E_{loc,i}(r_i),$$

$$i = 1, 2, ..., N, \tag{1}$$

where the local field $E_{loc,i}(r_i)$ is the sum of the field radiated from all the other N-1 dipoles. For a given wavelength λ, including the contribution of all the other dipoles, the local field can be written as

$$E_{loc,i}(r_i) = E_0 \exp(ik \cdot r_i) - \sum_{\substack{j=1 \\ i \ne j}}^{N} A_{ij} P_j,$$

$$i = 1, 2, ..., N, \tag{2}$$

where k and E_0 are the wave vector and the amplitude of the incident radiation, respectively. The contribution to the electric field at position i due to the dipole at position j is contained in the second term on the right side of (2) and is normally expressed in terms of the dipole-dipole interaction matrix A as

$$A_{ij} P_j = \frac{\exp(ikr_{ij})}{r_{ij}^3} \left\{ k^2 r_{ij} \times (r_{ij} \times P_j) + \frac{1 - ikr_{ij}}{r_{ij}^2} \times \left[r_{ij}^2 P_j - 3r_{ij}(r_{ij} \cdot P_j) \right] \right\}$$

$$i = 1, 2, ..., N, j = 1, 2, ..., N, j \ne i. \tag{3}$$

where r_{ij} and r_{ij} correspond to the dipole-dipole position difference vector and magnitude that are defined as $r_i - r_j$ and $\left| r_i - r_j \right|$, respectively. Substituting (2) and (3) into (1), we can generate the system of equations

$$A' \cdot P = E, \tag{4}$$

where the off diagonal elements of the matrix, A'_{ij} is the same as A_{ij}, and the diagonal elements of the matrix, A'_{ij} is α^{-1}.

For a system with N total dipoles, E and P are 3N-dimensional vectors, and A' is a $3N \times 3N$ matrix. Solving this set of 3N complex linear equations, the polarizations P_i are determined, and from this we can calculate cross section of the extinction as

$$C_{ext} = \frac{4\pi k}{\left| E_0 \right|^2} \sum_{i=1}^{N} \text{Im} \left(E_{loc,i}^* \cdot P \right)_i \tag{5}$$
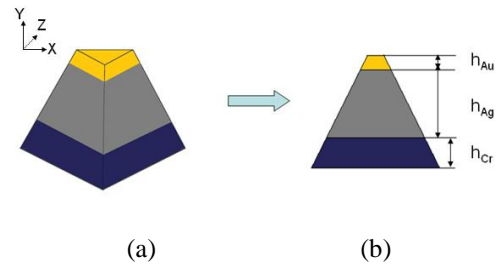

Fig. 1. (a) 3-D schematic view, (b) Cross section view of a single hybrid nanoparticle.
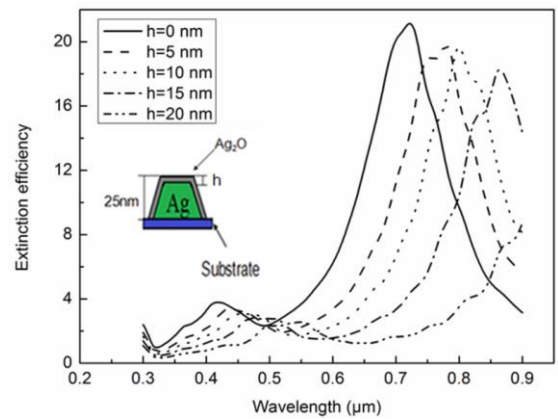

Fig. 2. Extinction spectra of the Ag nanostructure arrays with different Ag$_2$O layer thicknesses.
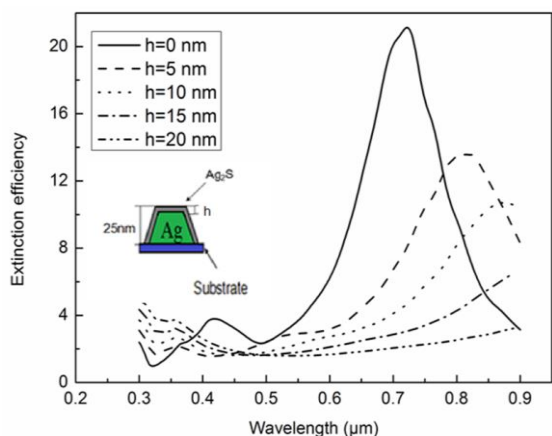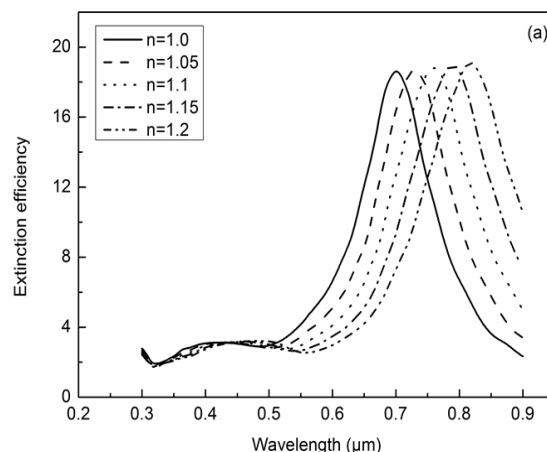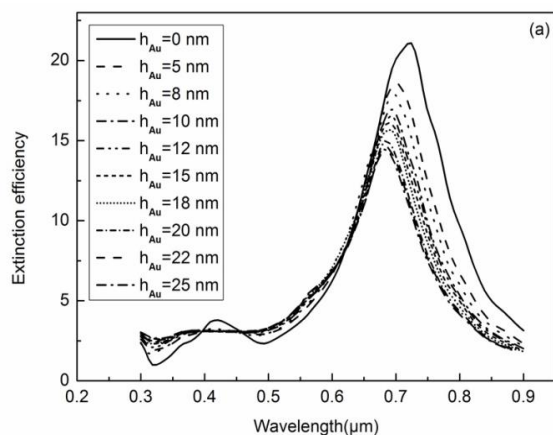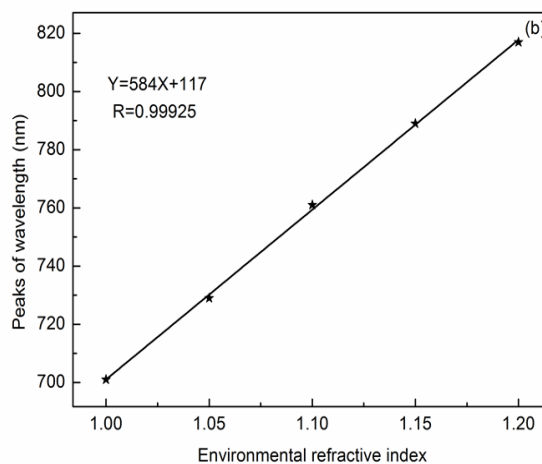
Fig. 3. Extinction spectra of the Ag nanostructure arrays with different Ag$_2$S layer thicknesses.
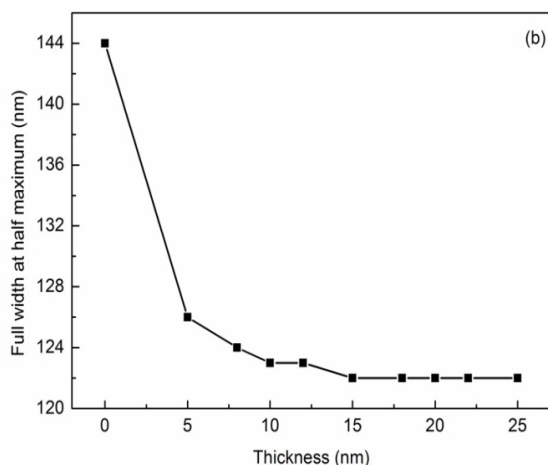

(a) Extinction spectra in different media for h$_{Au}$ =5 nm

(a) Extinction spectra for different thicknesses of the Au film

(b) Refractive index sensitivity curve for h$_{Au}$ = 5 nm

(b) Full width at half maximum as a function of the thickness of Au film

Fig. 4. Calculation results of the hybrid Au-Ag triangular nanostructure arrays with different Au layer thicknesses.
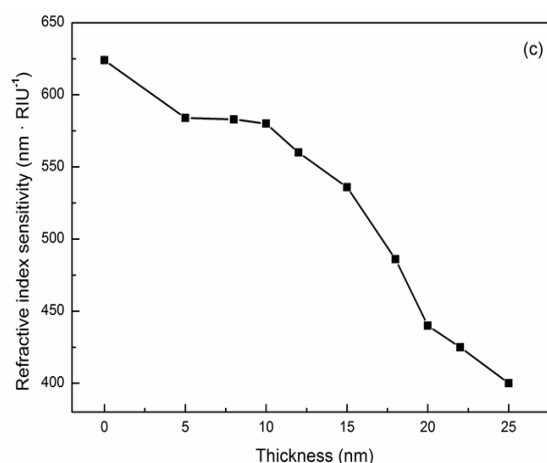
(c) Refractive index sensitivity distributions for different Au layer thicknesses

Fig. 5. Sensing performance of the hybrid Au-Ag triangular nanostructure arrays with different Au layer thicknesses.
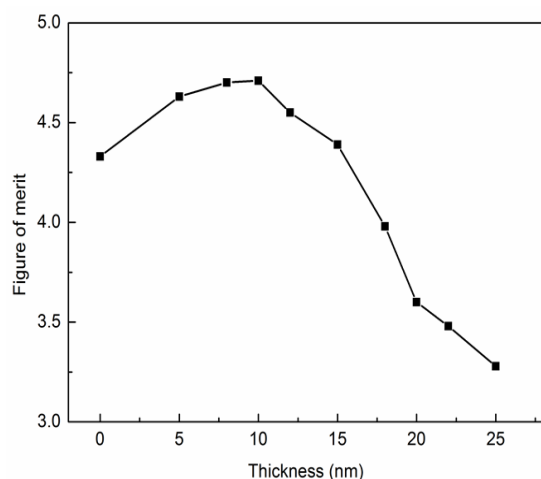
Fig. 6. Figure of merit of the hybrid Au-Ag triangular nanostructure arrays with different Au layer thicknesses.

3. Results and discussions

3.1 Effect of oxidation and sulfuration of Ag nanoparticles

The LSPR λ_{max} of metallic nanoparticles is sensitive not only to the size, shape, interparticle spacing, and the dielectric properties of the metal but also is quite sensitive to the dielectric environment surrounding the nanoparticles. In particular, the oxidation and sulfuration on surface of the Ag film is expected to result in an abnormal shift in LSPR λ_{max}. Extinction is a term used in physics to describe the absorption and scattering of electromagnetic radiation. Any changes in the parameters of metal nanoparticles could lead to the optical drift in extinction spectrum and thus influence the optical applications in practice [19-22].

To investigate the influence of the oxidation and sulfuration on the peak wavelength shift, we have performed DDA calculations for Ag nanoparticles whose total height is fixed at 25 nm and total width fixed at 180 nm, where we have replaced Ag by Ag_2O and Ag_2S in the top layer, respectively. The Ag_2O and Ag_2S layer have a thickness h varying from 5 to 20 nm. Fig. 2 shows the extinction spectra of triangular Ag nanostructure arrays with different Ag_2O layer thicknesses. Fig. 3 shows the extinction spectra of triangular Ag nanostructure arrays with different Ag_2S layer thicknesses. The obtained results show that the thicknesses of Ag_2O and Ag_2S layer have great influence on the extinction spectra. When the thickness is increased, the intensity of the extinction decreases while the peak positions of the extinction efficiency exhibits obviously red shifts. The dielectric constant of the Ag thin film has been definitely changed due to the oxidation and sulfuration. Moreover, it is noted, as can be seen from the extinction spectrum in Fig. 2, each curve has several peaks independent on the thickness of Ag_2O. This phenomenon not only relates to the Ag material, but also relates to the optical properties of triangular nanoparticle. For Ag triangular nanoprism, the extinction spectrum always shows several peaks due to the in-plane and out-of plane polarization [23].

3.2 Extinction spectra of the hybrid Au-Ag triangular nanostructure arrays

To overcome the oxidation and sulfuration, we concentrate on the hybrid Au-Ag triangular nanoparticle arrays. Using the DDA algorithm, we design and calculate the extinction spectra of the hybrid nanoparticles and corresponding model is shown in Fig. 1.

The out-of plane heights of the Ag nanoparticles under the Au layer is 25 nm and the top Au nanoparticles has a thickness h_{Au} varying from 5 to 25 nm. The in-plane widths of each nanoparticles is 180 nm. Fig. 4 shows calculation results of the hybrid Au-Ag triangular nanostructure arrays with different Au layer thicknesses. According to the calculated extinction spectra presented in Fig. 4, when the thickness of the Au layer is increased, the positions of the peak wavelengths appear slightly blue shifted while the intensity of the extinction has obviously been decreased. The full width at half maximum (FWHM) decreases rapidly with the thickness of Au layer increasing from 0 to 10 nm and then it decreases slowly with increasing Au layer thickness to 25 nm. As can be seen from Fig. 2 to 4, the hybrid Au-Ag triangular nanostructures array is good structure to tune the plasmon peak and have the high intensity of the extinction.

3.3 RIS of the hybrid Au-Ag nanostructure arrays

In order to investigate the effect of the Au layer thickness on the sensitivity of the hybrid Au-Ag triangular nanostructure arrays, we calculate the extinction spectra of the effective refractive index of the mediums surrounding the Au-Ag nanostructure array. The RIS is defined as $m=\Delta\lambda/\Delta n$ [24], where $\Delta\lambda$ and Δn denote the peak of the wavelength change and the refractive index change, respectively. For the hybrid nanostructure array with 5 nm Au layer thickness, the peak wavelength has a red shift when the refractive index n increases, as shown in Fig. 5a. For example, when the refractive index increases from 1.0 to 1.05, the peak wavelength shifts from 699 nm to 727 nm, exhibiting a RIS of 584 nm/RIU (refractive index unit), as indicated in Fig. 5 b. Fig. 5c shows the RIS of the Au-Ag triangular nanostructure arrays with different Au layer thicknesses.

From the calculated results, we can see that the thickness of the Au layer causes the change of the RIS of the hybrid Au-Ag nanostructure arrays. When the Au layer thickness increased from 0 to 5 nm and from 10 to 25 nm, RIS is decrease rapidly and appears a slow decline with the thickness of Au layer increasing from 5 to 10 nm. This result shows that when the thickness of Au layer varying from 5 to 10 nm, the RIS of the hybrid nanostructure keeps more stable and has a higher value.

3.4 FOM of the hybrid Au-Ag nanostructure arrays

The FOM for a metal nanostructure is defined as p=S/W [25], where S and W denote the RIS and FWHM, respectively. According to the Fig. 4b and Fig. 5c, we calculate the FOM and the calculation result is shown in Fig. 6.

It can be seen from Fig. 6 that the result shows that the FOM increases with the thickness of Au layer increasing from 0 to 10 nm and then decreases with increasing Au layer thickness to 25 nm. we can find that the maximum FOM is around 4.7, when the thickness of the Au layer is 10 nm.

4. Fabrication of nanostructure

Considering capability of the nanostructure fabrication in experiment, the Au and Ag layer thickness is selected as 10 nm and 25 nm, respectively, in the DDA calculation. In our experiments, the hybrid Au-Ag triangular nanostructure is fabricated by means of a NSL technique. The PS nanospheres with a mean diameter of 360 nm and a concentration of 10 wt% in solution are purchased from Suzhou Nano–Micro Bio-Tech Co. Ltd. First of all, closed-packed nanosphere is a prerequisite. The regular monolayer as a deposition mask is principal to achieve large-area hexagonal structure. To begin with, the PS solution is diluted to be 3wt% with deionized water. The glass substrates are firstly ultrasonic cleaned, in toluene, acetone, ethanol for 10 min respectively, and then in piranha solution (H_2SO_4 : H_2O_2 = 3:1) for 2 hours to remove organic residues. To achieve a hydrophilic surface, the glass substrates are ultrasonically bathed in NH_4OH, H_2O_2, and H_2O solution with the ratio of 1:1:5 for 2 hours. Every sonication followed rinsing with large amount of deionized water. The cleaned surstrates are stored in deionized water for used.

Following drop-coating of the PS nanospheres on the glass substrate, a Ag and Au layer, are deposited on the PS mask sequentially, as shown in Fig. 7. The hybrid Au-Ag particles can protect oxidation and sulfuration of the pure silver particles from ambient environment.

The deposition of there metallic layers (3N Au, 3N Ag) is performed in a home-built thermal evaporator at a pressure of 5.0×10^{-4} Pa. The substrates are rotated at a speeds of 16.5 rpm all through the deposition. To achieve homogeneous deposition, the power for heating up of the source materials is carefully increased. The deposition rate is ~ 2.5 nm/s for Au and Ag layers. The thickness had been monitored using a Dektak 3 Series surface profiler to achieve an identical depth for a low reflectance. It is controlled to be 10 nm for Au, and 25 nm for Ag films, respectively. After the deposition of Au film, the PS spheres are lifted off by immersing in absolute ethanol for about 5s. The PS are also removed by sonication (B3500S-MT, Branson, 140W, 42 kHz) in absolute ethanol. Nanostructures of the achieved PS mask and the

hybrid Au-Ag nanoparticle arrays are characterized by LEO-1530 SEM. Ultravioletvisible (UV-vis) mirror reflection spectra are obtained on a Varian Cary 5000 UV-Vis-NIR spectrophotometer.
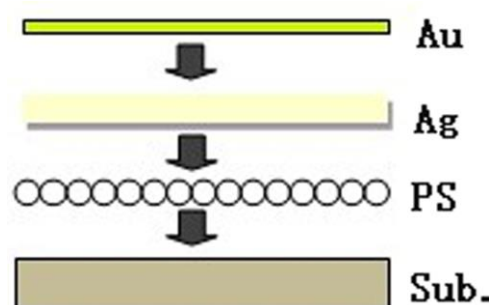

Fig. 7. Schematic illustration of hybrid Au-Ag nanoparticle array fabrication with this processes: the PS mask as an adhesive layer, Au thin film is deposited on top of the Ag film.

5. Testing results and discussion

Fig. 8 shows the SEM images of the hybrid Au-Ag triangular nanostructure array with 10 nm Au film. As showed in Fig. 8, the hybrid nanostructure array exhibits a uniform triangular structure and is arranged as a hexagonal array over a large scale area. The angular structure is regular and its tip is sharp. This structure is very conducive to further modification experiments for signal detection.
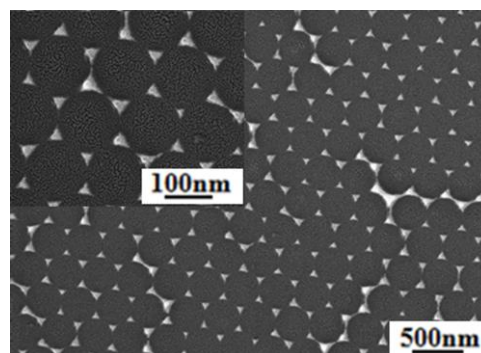

Fig. 8. The SEM images of the hybrid Au-Ag triangular nanostructure array with 10 nm Au film.

In our experiments, we detect the extinction efficiency of the representative the hybrid Au-Ag triangular nanoparticle arrays with 10 nm thickness of the Au film. The experimental and the calculated results are shown in Fig. 9. It can be seen apparently that when the wavelength is 669 nm, the extinction efficiency reaches to a maximum value. When DDA calculation is taken to calculate the extinction efficiency, the maximum wavelength of extinction efficiency is 697.3 nm, as shown in Fig. 9. The calculated result of the plasmon wavelength with the designed model agrees with recent experimental result. The only major difference with the experiment is that the

experimental peak is shifted by 28 nm to the blue compared to the calculated result. This is likely caused by substrate effect [26]. The other reason is that fabrication error causes uniformity issue for both size and shape of the particles. In addition, in DDA calculated model, the edge of the triangular nanoparticles is straight while in experiment it is curving. Most of the results presented here are analysis and characterization of the Au layer thickness variation. The results for the 2D hexagonally arranged hybrid Au-Ag triangular nanoparticle arrays show that the suitable Au film thickness is around 10 nm for our experimental fabrication. The experimental results are generally in agreement with the calculated results.
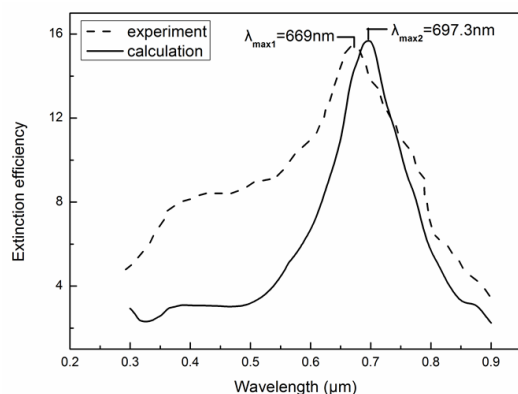

Fig. 9. Extinction spectra of experiment and calculation.

6. Conclusion

A hybrid Au-Ag triangular nanostructure array is come up with for the purpose of preventing oxidation and sulfuration occurring on Ag film surface. The Au layer thickness has significant effect on the optical properties and sensing performance of the hybrid nanostructure array. The calculation results by DDA numerical method demonstrate that the presence of the oxide layer and sulfide layer in Ag nanostructure is observed to cause an remarkable red shift of extinction spectra. When the thickness of Au and Ag are fixed on $h_{Au} = 10$ nm and $h_{Ag} = 25$ nm, It is found to possess the better RIS and FOM. After fabrication using NSL technique, spectroscopic results show that the measured spectrum is basically in agreement with the theoretical spectrum derived by the DDA calculation. The achieved structure can be used for detecting many species of biomolecules and drugs in the future.

References

[1] C. L. Haynes, A. D. McFarland, L. L. Zhao, R. P. Van Duyne, G. C. Schatz, J. Phys. Chem. A, **107**, 7337, (2003).
[2] C. L. Haynes, R. P. Van Duyne, Nano Lett., **3**, 939, (2003).
[3] P. C. Andersen, K. L. Rowlen, Appl. Spectrosc., **56**, 124A, (2002).
[4] Y. Q. Fu, W. Zhou, L. E. N. Lim, J. Opt. Soc. Am. A, **25**, 238 (2008).
[5] A. J. Haes, S. L. Zou, G. C. Schatz, R. P. Van Duyne, J. Phys. Chem. B, **108**, 109, (2004).
[6] J. Y. Liu, H. Yang, X. G. Luo, W. Y. Ma, Y. L. Liu, Acta Opt. Sin., **30**, 1092, (2010).
[7] Y. Q. Fu, W. Zhou, J. Nanophoton. (2009).
[8] S. L. Zhu, W. Zhou, J. Comput. Theor. Nanos., **3**, 634, (2010).
[9] G. K. Joshi, P. J. McClory, S. Dolai, R. Sardar, J. Mater. Chem., **22**, 923, (2012).
[10] J. S. Sekhon, H. K. Malik, S. S. Verma, Rsc Adv., **3**, 15427 (2013).
[11] B. Spackova, J. Homola, Opt. Express, **21**, 27490, (2013).
[12] G. H. Chan, J. Zhao, G. C. Schatz, R. P. Van Duyne, J. Phys. Chem. C, **112**, 13958 (2008).
[13] C. Novo, A. M. Funston, L. Pastoriza-Santos, L. M. Liz-Marzan, P. Mulvaney, J. Phys. Chem. C, **112**, 3 (2008).
[14] E. Martinsson, M. M. Shahjamali, K. Enander, F. Boey, C. Xue, D. Aili, B. Liedberg, J. Phys. Chem. C, **117**, 23148 (2013).
[15] R. Jin, Y. W. Cao, C. A. Mirkin, K. L. Kelly, G. C. Schatz, J. G. Zheng, Science, **294**, 1901 (2001).
[16] B. T. Draine, P. J. Flatau, J. Opt. Soc. Am. A, **11**, 1491 (1994).
[17] N. Felidj, J. Aubard, G. Levi, J. Chem. Phys., **111**, 1195 (1999).
[18] G. C. Schatz, J. Mol. Struc-Theochem, **573**, 73 (2001).
[19] S. Samanta, P. Sarkar, S. Pyne, G. P. Sahoo, A. Misra, J. Mol. Liq., **165**, 21 (2012).
[20] P. Sarkar, D. K. Bhui, H. Bar, G. P. Sahoo, S. Samanta, S. Pyne, A. Misra, Plasmonics, **6**, 43 (2011).
[21] L. P. Jiang, S. Xu, J. M. Zhu, J. Zhang, H. Chen, Inorg. Chem., **43**, 5877 (2004).
[22] B. Tang, J. An, X. L. Zheng, S. P. Xu, D. M. Li, J. Zhou, B. Zhao, W. Q. Xu, J. Phys. Chem. C, **112**, 18361 (2008).
[23] K. L. Kelly, E. Coronado, L. L. Zhao, G. C. Schatz, J. Phys. Chem. B, **107**, 668 (2003).
[24] S. L. Zhu, C. L. Du, Y. Q. Fu, Optical Materials. **31**, 1608 (2009).
[25] L. J. Sherry, S. H. Chang, G. C. Schatz, R. P. Van Duyne, Nano Lett., **5**, 2034 (2005).
[26] P. C. Chaumet, A. Rahmani, G. W. Bryant, Phys. Rev. B, **67** (2005).

*Corresponding author: jingliu@jmu.edu.cn